RSC Advances

PAPER

View Article Online
View Journal | View Issue

Cite this: *RSC Adv.*, 2025, **15**, 46761

Levels of polycyclic aromatic hydrocarbons around a scrap iron and steel recycling industry and the associated health risk assessment

Olusola Adedayo Adesina, *[a] Oluwatomi Atinuke Fakayode,*[a] Mufliah Gbemisola Omofoyewa,*[a] Khairia Mohammed Al-Ahmary,*[b] Saedah R. Al-Mhyawi,*[c] Ibtehaj F. Alshdoukhi*[d] and Sarah Bader alotaibi*[e]

The recycling of iron and steel is among the booming sectors in the Sub-Saharan countries of Africa. However, these industries generate different air pollutants due to inadequate control devices and a lack of monitoring by government control agencies. In this study, the levels of ambient air concentration and distribution of PAHs around a steel and iron scrap melting industry were investigated. Health indices including the incremental lifetime cancer risk (ILCR) and hazard quotient (HQ) were utilized to access the potential health effects of human exposure to PAHs in the ambient air surrounding this facility. The PAHs in the ambient air were collected using passive samplers in accordance with the procedures outlined in the South Pacific Regional Project's Annex 3. The quantification of PAHs was done using GC-MS. The results showed that the $\sum$ PAHs ranged from 49.6 to 530.1 pg m^{-3} in the dry season and 27.5 to 498.6 pg m^{-3} in the wet season. The $\sum$ carcinogenic PAHs ranged from 2.5 to 115.7 pg m^{-3} in the dry season and 1.7 to 28.6 pg m^{-3} in the wet season. The average ILCR for the wet season was 1.5×10^{-5} for children and 1.33×10^{-5} for adults, while for the dry season, the mean ILCR values were 2.7×10^{-5} for adults and 2.4×10^{-5} for children. Additionally, there was a considerable noncarcinogenic risk shown by the calculated hazard quotient, which was several times greater than that of the permissible limit of 1. The analysis quantified the concentrations of PAHs in the vicinity of the scrap iron and steel company and recommended the use of modern air control devices to control air emissions.

Received 21st July 2025
Accepted 5th November 2025

DOI: 10.1039/d5ra05266a

rsc.li/rsc-advances

Introduction

The ambient air quality is of global concern as nine out of ten people around the world breathe polluted air.[1] Additionally, millions of untimely deaths are recorded yearly from air pollution-related diseases.[1,2] It is even more concerning in countries of Africa, where there is no proper inventory on the various sources of air pollution in the environment. A study[3] has shown that the cases of premature deaths caused by air pollution exceed the cases recorded from malaria and HIV/AIDS.

The iron and steel smelting industries are one of the contributors to air pollution in Africa, which are less investigated. These industries have been expanding in the country due to the availability of scrap metals and the growing demand for iron rods.[4] Nigeria consumes 6.8 million metric tons of steel each year, and the precise amount of scrap metal generated in the country is still unknown due to inadequate data collection and management.[5]

In order to reduce environmental pollution caused by the littering of the scrap metals, recycling becomes inevitable.[6] Scrap metal recycling plants have been established in different parts of the country to reduce environmental degradation and for the value addition of these products. However, no proper monitoring is being done to regulate the activities of these industries in the country. Heavy smoke is usually seen getting emitted into the ambient air during the production hours of these industries, creating concerns regarding air pollution. The basic techniques and processes of iron and steel smelting involve raw molding, high-temperature melting, and casting.[7] However, these processes are associated with the generation of a significant amount of air contaminants due to inadequate control devices in their production processes.[8]

PAHs are emitted from both natural and anthropogenic sources and a majority of the PAHs released into the

[a]*Department of Chemical Engineering, Afe-Babalola University, Ado-Ekiti, Ekiti State, Nigeria. E-mail: adesinaolusola50@yahoo.com; fakayode.olutomi@gmail.com; gomofoyewa@gmail.com*

[b]*Department of Chemistry, College of Science, University of Jeddah, Jeddah, Saudi Arabia. E-mail: kmal-ahmary@uj.edu.sa*

[c]*Department of Chemistry, College of Science, University of Jeddah, Jeddah, Saudi Arabia. E-mail: sral-mhyawi@uj.edu.sa*

[d]*Department of Basic Sciences, College of Science and Health Professions, King Saud bin Abdulaziz University for Health Science, King Abdullah International Medical Research Centre, Riyadh, Saudi Arabia. E-mail: Alshdoukhii@ksau-hs.edu.sa*

[e]*Department of Teaching and Learning, College of Education and Human Development, Princess Nourah bint Abdulrahman University, P.O. Box 84428, Riyadh, 11671, Saudi Arabia. E-mail: Sbalotaibi@pnu.edu.sa*

environment are basically from these sources.[9] There has been an increase in awareness of these pollutants due to their carcinogenic potential, toxicity, and teratogenic properties.[9,10] PAHs are emitted into the air as by-products of incomplete combustion processes, the burning of bio-organic matter, automobile exhaust emissions, and industrial emissions.[11–14] Few studies are available on ambient air contamination from activities related to scrap iron and steel recycling, especially in Sub-Saharan Africa, where there is air contamination associated with heavy metals and particulate matter.[15–18] Few studies are available on the emission of PAHs from scrap iron and steel recycle plants, which encouraged this investigation.

Additionally, there are no regulations and guidelines in place in the country for regulating the ambient air emission of PAHs from these industries. Hence, this study focuses on the determination of ambient concentration levels and the distribution of PAHs around a scrap iron and steel recycling facility. This study also determined the risk associated with human exposure to PAHs around the vicinity using some health indices.

Materials and methods

Study area

This research was conducted in the area surrounding a metal recycling plant situated along the Osogbo–Ikirun Highway, approximately 3.5 km from Osogbo, the capital of Osun State, Nigeria. Fig. 1 displays the map indicating the sampling sites around the plant's location. Thirteen sampling points were chosen based on the predominant wind direction and most importantly, the sampling points were in the vicinity of residential buildings around the perimeter of the recycling plant, allowing for the determination of human exposure to these pollutants. The sampling was done for two seasons (wet and dry) in 2023.

Sampling

The sampling was done using a modified technique in Annex 3 of South Pacific Regional Project for Passive Air Sampling.[19,20] The passive sampler consisted of two stainless-steel bowl sizes (30 cm and 24 cm) and polyurethane filters (PUF). The PUF filters were configured with a 14-cm diameter, thickness of 1.35 cm, a 365-cm^2 surface area, and a density of 0.030 g cm^{-3}. Before deployment, the PUF disks were washed with distilled water and then rinsed in a Soxhlet extractor with acetone and petroleum ether for a whole day.[21]

On deployment, each sampler was placed on an iron rod (2 m) above the ground. The sampling was done for 28 days and then the samples were transported to the laboratory for analysis. The PAHs were extracted from the PUF discs in a Soxhlet

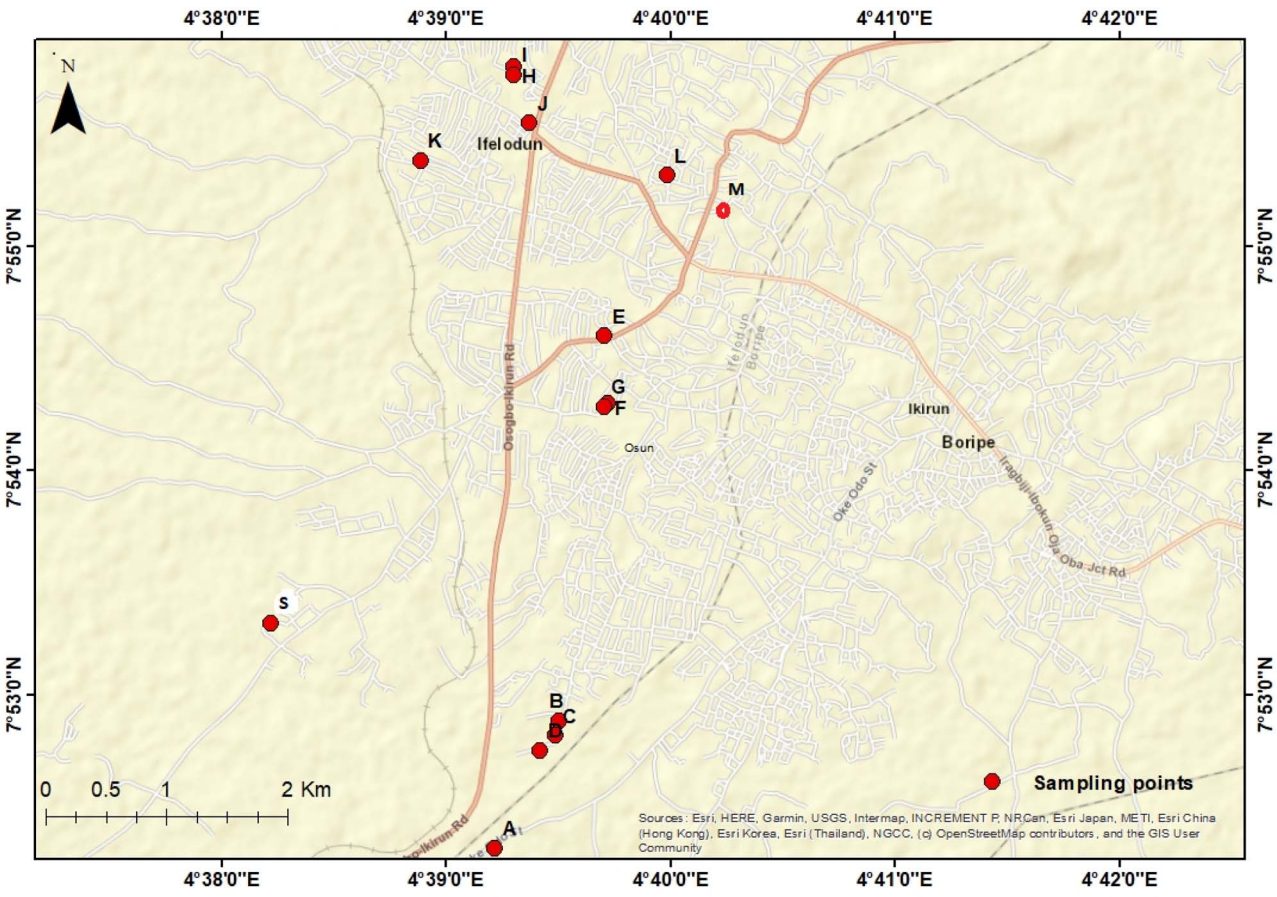

Fig. 1 Map of sampling locations (source: ArcGIS, https://www.arcgis.com/apps/mapviewer/index.html?webmap=6aa1b2a1bb7e4606adbd539528dcb1db).

extractor using dichloromethane (Sigma-Aldrich). The temperature for extraction was set at 60 °C for seven hours.[14] The extract was refined in open glass columns using liquid–solid adsorption chromatography with alumina and silica (200–400 mesh, Zico-Tech) as adsorbents. The extracts were concentrated using rotary evaporator (Infitex Co., Ltd).

PAHs analysis

PAHs were quantified using a GC-MS/MS 4000/3800 gas chromatograph (Agilent Technologies, Pato Alto, CA) with a fixed stationary-phase thickness, a chosen ion monitoring mode and a 1 m column (dimension of 60 m × 0.32 mm). Nitrogen was employed as the carrier gas. The GC was operated in a splitless mode at a temperature of 250 °C. The initial column temperature was 70 °C, at 10 °C min^{-1} to 260 °C. It was increased to 300 °C min^{-1} for 8 min. The solvent delay was 7 min, and a dwell time of 0.1 s was used for each *m/z* value. The MS transfer line was maintained at 250 °C, and quantification was based on calibration with the standard analyte using the mass spectrometer in the selective ion monitoring (SIM) mode. Adesina *et al.*[14] have reported on the GC-MS condition that was utilized. Using the proper mathematical ratios, the PAH compounds were subjected to source identification and diagnosis. The quantification of the constituent PAHs was done using external standard methods (PAH mix, Sigma Aldrich, 10 μg ml^{-1}).

QA/QC

The samples were collected in duplicates, and the field and lab blanks were processed alongside the samples. No blank corrections were required since PAH levels in the field blanks were below the detection threshold for all the targeted PAH compounds. Each sample was spiked with 20 ng of phenanthrene-d10 as a recovery standard (RS) before extraction, yielding PAH recoveries between 85% and 93%. The limit of detection (LOD), limit of quantification (LOQ), recovery (%), and relative standard deviation (RSD, %) were calculated to ensure the integrity of the data. The LOD and LOQ values for the PAHs were determined based on the ratio value of the signal-to-noise baseline (S/N)[22]. The values for the limit of detection (LOD), limit of quantification (LOQ), recovery (%), and relative standard deviation (RSD, %) are shown in Table 1.

Data analysis

The air volume captured by each PUF disk was determined using the Global Atmospheric Passive Sampling (GAPS) network model.[20,23] The input data included deployment duration, surrounding temperature, and a sampling rate of 4 m^3 per day.[20,24] Descriptive and inferential statistics were employed to examine the collected data. The principal component analysis (PCA) and hierarchical clustering (HCA) were used to analyze the patterns in the data obtained, while spatial distribution was done using the geostatistical interpolation technique to create a continuous map using the ordinary Kriging algorithm.

Table 1 LOD, LOQ, recovery and RSD values (pg m^{-3}) of PAHs

Target compound	LOD	LOQ	Recoveries (%)	RSD
Nap	0.2	0.32	91	9.1
Acy	0.21	0.32	95	8.9
Acen	0.12	0.21	92	8.2
Fln	0.1	0.19	87	7.8
Phe	0.12	0.24	86	7.6
Ant	0.14	0.23	95	8.9
Flt	0.14	0.31	95	8.2
Pyr	0.18	0.21	95	9.2
BaA	0.19	0.25	93	8.6
CHR	0.16	0.31	92	9.1
Bbf	0.21	0.31	95	9.2
Bfk	0.12	0.29	94	8.4
Bap	0.15	0.31	90	8.2
Icp	0.13	0.27	92	9.1
DHa	0.15	0.23	94	9.2
Bgp	0.12	0.31	94	9.2

Risk assessment

Toxicity equivalent (TEQ) for PAHs

The possible toxicity of the PAHs found in the samples was estimated using the toxicity equivalency factor (TEF). The TEFs for each polycyclic aromatic hydrocarbon (PAH) were calculated by multiplying the corresponding concentration of the PAH by its TEF.

Hazard quotient and incremental lifetime cancer risk

The hazard quotient and incremental lifetime cancer risk (ILCR) were calculated using eqn (i) and (ii), respectively:[14,25]

$$\mathrm{ILCR_{Inh}} = \frac{C \times \mathrm{IR} \times \mathrm{ED} \times \mathrm{EF} \times \mathrm{IUR}}{\mathrm{AT} \times \mathrm{BW}} \quad \text{(i)}$$

$$\mathrm{HQ} = \frac{C \times \mathrm{IR} \times \mathrm{ED} \times \mathrm{EF}}{\mathrm{AT} \times \mathrm{BW} \times \mathrm{RfD}} \quad \text{(ii)}$$

The concentration of the PAHs (μg m^{-3}) is represented by *C* in this study. The inhalation rate (IhR) of 20 m^3 per day for adults and 9.6 m^3 per day for children was used. The exposure duration (20 years) was used because the industry was established 20 years ago. The exposure frequency was represented by EF as 365 days per year. The average exposure time was represented by AT in days. The people in the area are thought to be exposed to the emissions every day, or 365 days a year, with a life expectancy of 70 years, or 25 550 days. The inhalation risk, or IUR, is a risk factor for cancer; the WHO reports it to be 8.7×10^{-2} and the USEPA reports it to be 6×10^{-4}. The weight at birth (WB) was set to 70 kg, or 30 kg for children. The reference dosage concentration (RfC) used for the PAHs was 2×10^{-3} μg m^{-3}.

Results and discussion

Air samples collected from the area surrounding the scrap iron recycling plant were tested for 16 priority PAHs identified

Table 2 Concentration of PAHs in the dry season (pg m^{-3})

PAHs	A	Std	B	Std	C	Std	D	Std	E	Std	F	Std	G	Std	H	Std	I	Std	J	Std	K	Std	L	Std	M	Std
Nap	0	0	6.7	0.05	0	0	23.3	1	10	0.05	6.7	0.06	13.3	0.07	16.7	0.07	6.7	0.05	3.3	0.05	406.7	10	0	0	0	0
Acy	0	0	0	0	0.4	0.02	1.4	0.02	0.3	0.01	0	0	117	3	1.1	0.03	1.1	0.02	1.1	0.03	0	0	27.7	1	0.3	0.02
Ace	2.2	0.04	58.3	0.1	1.7	0.03	2.2	0.05	1.1	0.03	57.8	0.12	5	0.03	5	0.04	2.2	0.03	54.4	0.12	62.2	0.2	3.3	0.05	0.6	0.03
Fln	77.6	0.27	2.4	0.04	50	0.25	48.6	1.5	54.8	0.1	0.5	0.03	0	0	0	0	1	0.01	0	0	54.8	0.1	2.4	0	2.9	0.06
Phe	1.3	0.03	0.2	0.01	0	0	1.1	0.05	0.7	0.02	21.6	1	0	0	0	0	0.5	0.02	18	0.08	1.6	0.03	0	0	1.3	0.05
Pyr	11.4	0.05	0.2	0.01	0.3	0.01	0.7	0.03	0.3	0.01	0.5	0.03	10.1	0.05	10	0.05	0.2	0.01	0.1	0.01	0.8	0.02	0.1	0.01	0.1	0.01
Flt	12.6	0.05	0.4	0.02	0.8	0.02	0.4	0.02	0.2	0.01	11.4	0.07	0.5	0.02	0.9	0.04	0.5	0.02	0	0	0	0	0	0	0.2	0.01
Ant	19.5	0.05	1.6	0.03	0.7	0.02	0.5	0.03	0.5	0.02	1.3	0.04	0.2	0.01	0.2	0.01	0.5	0.03	20.2	1	1.5	0.03	19	0.08	0.9	0.03
B[*k*]F	0	0	9.7	0.05	0.6	0.02	1	0.05	0.5	0.02	0.3	0.02	0.4	0.02	0.4	0.02	0.5	0.01	0.2	0.01	0.6	0.02	0.6	0.03	0	0
B[*a*]P	0.1	0.01	0.5	0.02	11.4	0.05	8.9	0.06	10.2	0.05	0.2	0.02	0	0	0.1	0.01	0.3	0.01	10.3	0.05	0.4	0.01	0.2	0.01	0.7	0.03
CHR	11.1	0.05	0.9	0.02	10.3	0.05	10.1	0.07	9.9	0.04	10.6	0.06	10.5	0.06	9.5	0.05	10.2	0.05	0	0	0.2	0.01	0.8	0.04	10.2	0.05
B[*a*]A	0	0	0.8	0.02	92.3	0.3	0.6	0.02	10.7	0.05	9.5	0.05	0.5	0.03	0.7	0.02	9.2	0.04	0.8	0.04	0.2	0.01	11.4	0.05	10.4	0.05
IcP	0	0	0.1	0.01	0.7	0.02	0.8	0.03	0.6	0.02	0	0	0.8	0.04	0.9	0.03	11.3	0.06	0	0	0.4	0.02	9.7	0.04	0.2	0.01 s
B[*b*]F	0.1	0.01	0.7	0.02	0	0	0.5	0.02	10.5	0.05	0.7	0.03	9.8	0.05	0.6	0.02	0.2	0.01	0.5	0.03	0.3	0.01	9.7	0.04	10.3	0.05
DhA	0.1	0.01	0.6	0.02	0.4	0.02	0.4	0.01	0.3	0.01	0.3	0.02	0.7	0.04	8.8	0.04	0.5	0.02	0.4	0.02	0.4	0.02	9.1	0.04	0.5	0.02
BgP	0.4	0.02	0.9	0.02	0.3	0.01	0	0	0.3	0.01	0.2	0.02	9.6	0.05	9.1	0.05	10.4	0.05	0.3	0.01	0	0	0.1	0.01	11	0.06
∑carc	11.4	0.08	13.3	0.16	115.7	0.46	22.3	0.26	42.7	0.24	21.6	0.2	22.7	0.24	21	0.19	32.2	0.2	12.2	0.15	2.5	0.1	41.5	0.25	32.3	0.2
∑PAHs	136.4	0.59	84	0.44	169.9	0.82	100.5	2.96	110.9	0.5	121.6	1.57	178.4	3.47	64	0.48	55.3	0.44	109.6	1.45	530.1	10.48	94.1	1.4	49.6	0.47

by the EPA. The 16 priority PAHs are recognized as toxic, potentially carcinogenic, and ubiquitous in the environment, making them a significant concern for human and ecological health. These PAHs are acenaphthene (Ace), acenaphthalene (Acy), fluorene (Fln), anthracene (Ant), benz[*a*]anthracene (BaA), benzo[*a*]pyrene (BaP), benzo[*b*]fluoranthene (BbF), benzo[*ghi*]perylene (BgP), benzo[*k*]fluoranthene (BkF), chrysene (CHR), dibenz[*a*,*h*]anthracene (DhA), indeno[1,2,3 *cd*]pyrene (IcP), pyrene (Pyr), phenanthrene (Phe), fluoranthene (Flt), naphthalene (Naph). The concentration of PAHs at various locations is presented in Table 2 and Table 3. The highest concentration of Naph was observed in the dry season, ranging from 0 to 406.7 pg m^{-3}, with an average concentration of 38.0 pg m^{-3}. Other compounds with elevated levels include Fln, Ace, and Acy, with mean concentrations of 22.7, 19.7, and 11.5 pg m^{-3}, respectively. This can be attributed to their low molecular weight, which makes them more easily produced during combustion processes.[19,20] During the wet season, Nap and Fln were the most prevalent compounds in the air around the recycling plant, with concentrations of 40.3 pg m^{-3} and 42.04 pg m^{-3}, respectively. However, the lowest PAH concentrations observed for the dry season were Bkf, DhA, and Icp with mean concentrations of 1.14, 1.7, and 1.96 pg m^{-3}, respectively, while the lowest concentrations observed for the wet season are CHR and BgP. Because these compounds are high-molecular-weight PAHs, they are usually in the particulate phase and easily deposited onto the ground due to the influence of gravitational forces. This could be the reason for the low concentration of these compounds in the ambient air around the vicinity of the factory. There was a distinction between the ∑PAHs at the sampling locations between the wet and dry seasons (Fig. 2). The highest ∑PAHs of 530.1 pg m^{-3} were observed at Sampling Point K in the dry season, while the highest concentration of 498.6 pg m^{-3} was observed at Sampling Point G in the wet season. These observations are connected to variations in the predominant wind direction of this season. Although there are no data available for PAH emission into ambient air from scraped iron and steel recycling in Sub-Saharan Africa, the summation of PAHs observed in this study is higher than the results of Khaparde *et al.*[26] for integrated iron and steel plant emissions in India but lower than the observations of Liu *et al.*[9] on PAHs emitted from e-waste dismantling processes in Southern China.

The carcinogenic PAHs are (benz[*a*]anthracene (BaA), benzo[*a*]pyrene (BaP), benzo[*k*]fluoranthene (BkF), chrysene (CHR), benzo[*b*]fluoranthene (BbF), dibenz[*a*,*h*]anthracene (DhA), and indeno[1,2,3 *cd*]pyrene (IcP)). Among these PAHs, Bap is the most carcinogenic and it is an indicator of PAH contamination. During the dry season, the Bap concentrations ranged from 0 to 11.4 pg m^{-3}, with an average concentration of 3.30 pg m^{-3}. In the wet season, the concentration varied from 0 to 12.1 pg m^{-3}, with a mean of 1.89 pg m^{-3}. Fig. 3 illustrates the total carcinogenic PAHs at different sampling points, showing that the carcinogenic PAH levels were generally higher in the dry season than in the wet season. This difference could be largely attributed to wind speed and direction.

Table 3 Concentration of PAHs in the wet season (pg m^{-3})

PAHs	A	Std	B	Std	C	Std	D	Std	E	Std	F	Std	G	Std	H	Std	I	Std	J	Std	K	Std	L	Std	M	Std
Nap	13.3	0.07	23.3	1	0	0	350	10	20	0.08	20	1	26.7	1	23.3	0.09	6.7	0.08	6.7	0.09	6.7	0.06	13.3	0.07	13.3	0.06
Acy	0.6	0.03	0	0	0	0	0.5	0.02	0	0	0	0	0	0	0	0	2.1	0.06	2.4	0.04	2.4	0.03	2.1	0.04	1.3	0.03
Ace	2.5	0.04	0	0	0	0	0	0	2.5	0.05	3.5	0.03	5	0.04	2.5	0.03	3	0.06	3	0.05	4	0.04	3	0.05	4.5	0.05
Fln	5	0.05	5	0.04	3.2	0.04	51.4	1.4	5.5	0.06	4.5	0.05	450	8	5.9	0.04	3.7	0.04	3.2	0	3.2	0.05	3.2	0.06	2.7	0.05
Phe	0	0	0	0	1.4	0.02	0.2	0.01	0	0	0.3	0.02	0.5	0.02	0.5	0.03	3.4	0.05	16.6	0.09	19	0.08	18.8	0.08	18.3	0.08
Pyr	0.9	0.03	0.9	0.03	10.4	0.05	0.1	0.01	0.5	0.03	0.2	0.01	0.3	0.02	0.3	0.01	12.2	0.09	12.4	0.06	12.4	0.06	13.2	0.06	0.3	0.01
Flt	0	0	0.2	0.01	9.7	0.05	0.3	0.01	1.2	0.04	13.4	0.09	13.5	0.07	13.5	0.06	0.2	0.01	0.3	0.01	0.2	0.01	0.4	0.02	0.3	0.01
Ant	0	0	25.8	1	0	0	0	0	0.8	0.03	0.5	0.03	0.5	0.02	0	0	1.7	0.06	0.7	0.03	2.4	0.03	1.7	0.04	1	0.05
B[*k*]F	12.2	0.06	0.4	0.02	8.8	0.06	0	0	0.2	0.01	0.2	0.01	0.1	0.01	0.1	0.01	0.5	0.02	0.8	0.04	0.3	0.01	0.5	0.02	9.7	0.05
B[*a*]P	0.4	0.02	0.4	0.02	0.8	0.02	8.8	0.04	12.1	0.06	0.3	0.02	0.1	0.01	0.1	0.01	0	0	0.6	0.02	0	0	0	0	0.7	0.04
CHR	0.3	0.01	0.3	0.01	0.1	0.01	0.5	0.02	0.5	0.02	0	0	0	0	0	0	0.8	0.04	0.3	0.01	0.8	0.03	0.6	0.03	0.1	0.01
B[*a*]A	0.4	0.02	0.1	0.01	0	ND	9.1	0.04	0.1	0.01	11.7	0.08	12	0.06	12	0.05	1.1	0.05	0	0	0.6	0.03	0.7	0.03	0	ND
IcP	0	0	0	0	0.7	0.03	12	0.05	0.3	0.02	0	0	0	0	0	0	0.6	0.03	0.8	0.04	0.3	0.02	0.5	0.02	0.8	0.04
B[*b*]F	11.2	0.05	11.2	0.05	0.4	0.02	0.2	0.01	0	0	11.5	0.08	16.6	0.08	16.6	0.06	0.1	0.01	0	0	0.1	0.01	0.4	0.02	0	ND
DhA	0.4	0.02	10.9	0.05	0.4	0.02	0.3	0.02	12	0.07	0	0	0	0	0	0	0.1	0.01	0.3	0.02	0.2	0.01	0	0	0.5	0.03
BgP	0.1	0.01	0.1	0.01	0.1	0.01	0.2	0.01	0	0	0	0	0	0	0	0	0.1	0.01	0.7	0.04	0.3	0.01	0.3	0.01	0.3	0.02
∑carc	24.9	0.18	23.3	0.16	11.2	0.16	30.9	0.18	25.2	0.19	23.7	0.19	28.8	0.16	28.8	0.13	3.2	0.16	2.8	0.13	2.3	0.11	2.7	0.12	11.8	0.17
∑PAHs	47.3	0.41	78.6	2.25	36	0.33	433.6	11.64	55.7	0.48	66.1	1.42	525.3	9.33	74.8	0.39	36.3	0.62	48.8	0.54	52.9	0.48	58.7	0.55	53.8	0.53

Dry

PAH ratio	Source type	Value range	This study
Flu/(Flu + Pyr)	Petrogenic	<0.40	0.04–0.4 (2)
	Combustion source	>0.50	0.4–0.95 (9)
	Traffic emission	0.4–0.5	0.4–0.5 (2)
Ant/(Ant + Phe)	Petrogenic	<0.10	0.06–0.1 (1)
	Pyrogenic	>0.10	0.1–1.0 (12)
BaA/(BaA + Chr)	Petrogenic	<0.20	0.05–0.2 (2)
	Combustion	>0.35	0.35–0.93 (13)
	Mixed petrogenic and combustion	0.2–0.35	

Wet

PAH ratio	Source type	Value range	This study
Flu/(Flu + Pyr)	Petrogenic	<0.40	0.01–0.4 (5)
	Combustion source	>0.50	0.5–1.0 (8)
	Traffic emission	0.4–0.5	
Ant/(Ant + Phe)	Petrogenic	<0.10	0.04–0.1 (2)
	Pyrogenic	>0.10	0.1–1.0 (13)
BaA/(BaA + Chr)	Petrogenic	<0.20	0.1–0.2 (3)
	Combustion	>0.35	0.35–0.9 (9)
	Mixed petrogenic and combustion	0.2–0.35	0.2–0.35 (1)

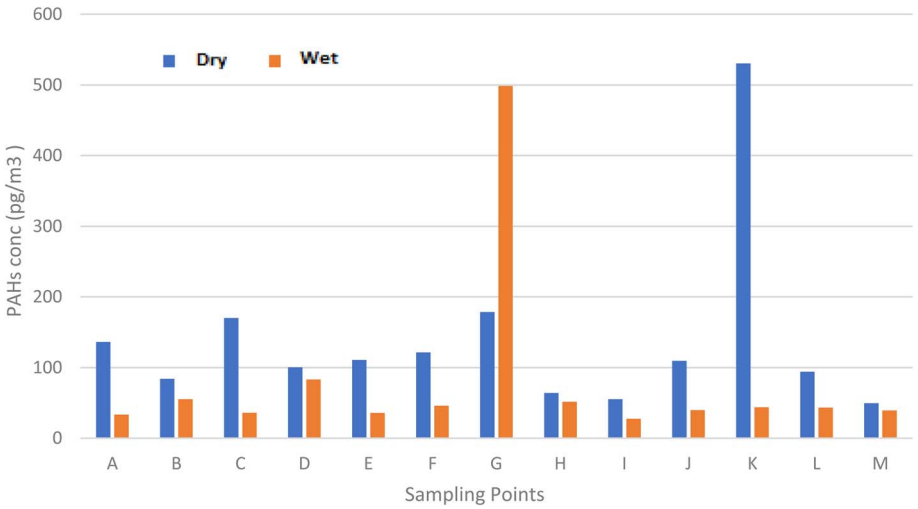

Fig. 2 PAH Summation at Sampling Locations.

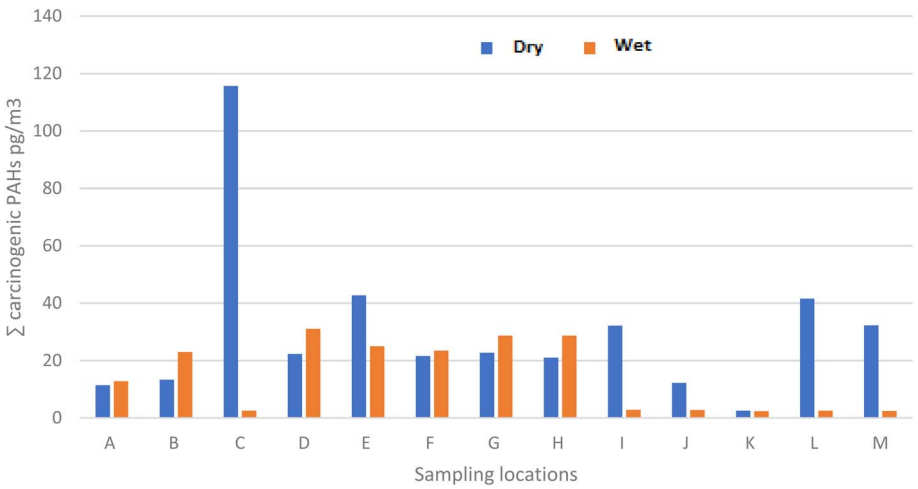

Fig. 3 Carcinogenic PAHs Summation at Sampling Locations.

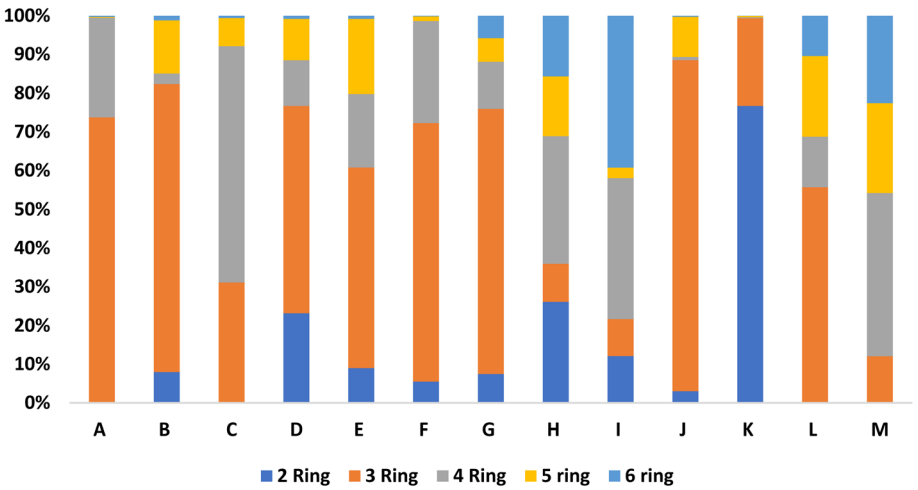

Fig. 4 Distribution of PAHs Based on the Number of Rings for the Wet Season.

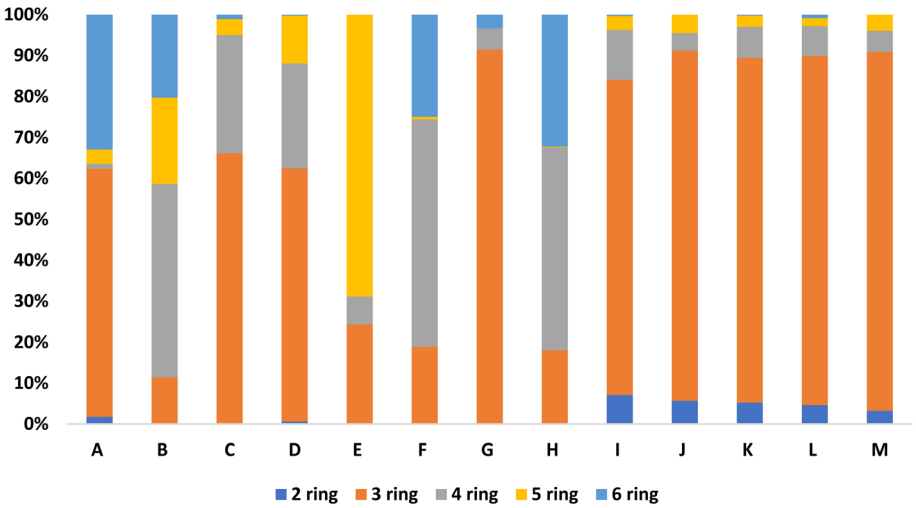

Fig. 5 Distribution of PAHs Based on the Number of Rings for the Dry Season.

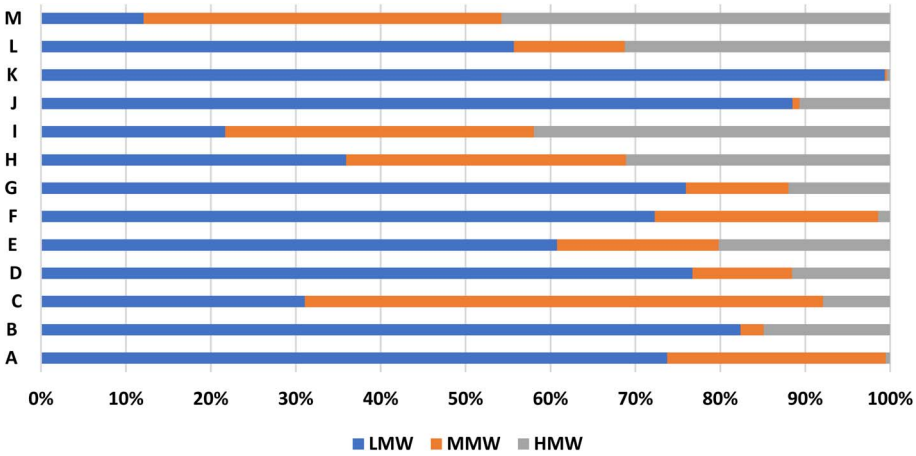

Fig. 6 Distribution of PAHs based on the molecular Weight for the dry season.

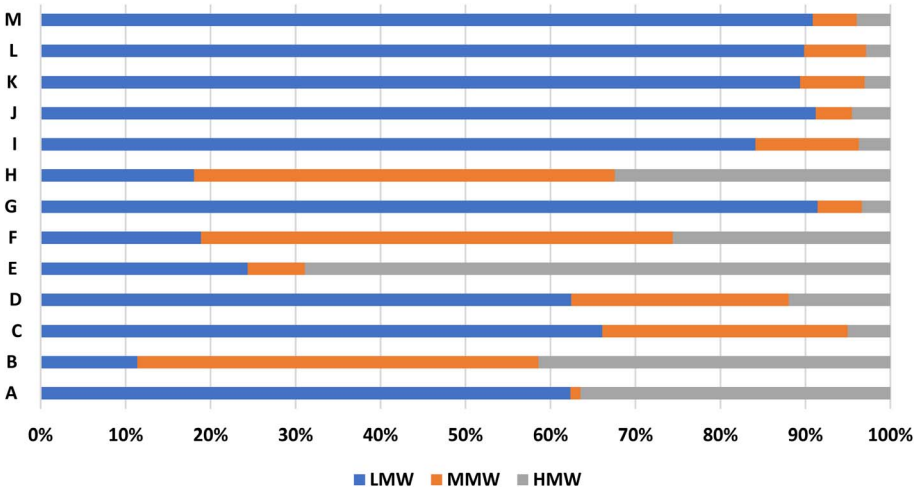

Fig. 7 Distribution of PAHs based on the molecular weight for the wet season.

Additionally, hydrological conditions can cause variability in PAH levels in the ambient air samples in this season. Precipitation during the wet season can remove PAHs from the air, leading to decreased concentrations.

Fig. 4 and 5 present the distribution of PAHs according to their ring structures during the dry and wet seasons, respectively. The 2-ring PAHs include Nap, while the 3-ring PAHs consist of Ace, Anth, Acy, Phen, and Flu. The 4-ring PAHs comprise BaA, Flt, Chr, and Pyr, while the 5-ring PAHs include BaP, BbF, DahA and BkF. The 6-ring PAHs are BgP and IcP. The 3-ring PAHs dominated in both seasons, ranging from 6% to 90% during the dry season and 11% to 91% during the wet season. This indicates that the emissions near the scrap iron recycling facility are primarily present in the gaseous phase. On the other hand, the 6-ring PAHs were the least prevalent in both seasons, likely due to their heavy nature, which limited their dispersion. PAHs can also be classified by their molecular weight: low-molecular-weight (LMW) PAHs consist of 2- and 3-ring compounds, middle-molecular-weight (MMW) PAHs include 4-ring compounds, and high molecular weight (HMW) PAHs consist of 5- and 6-ring compounds.[27,28] Fig. 6 and 7 depict the distribution of PAHs based on their molecular weight for both the dry and wet seasons. It was observed that the low-molecular-weight PAHs were the most dominant for both seasons, confirming that the PAHs emitted around this facility were in the gaseous phase.

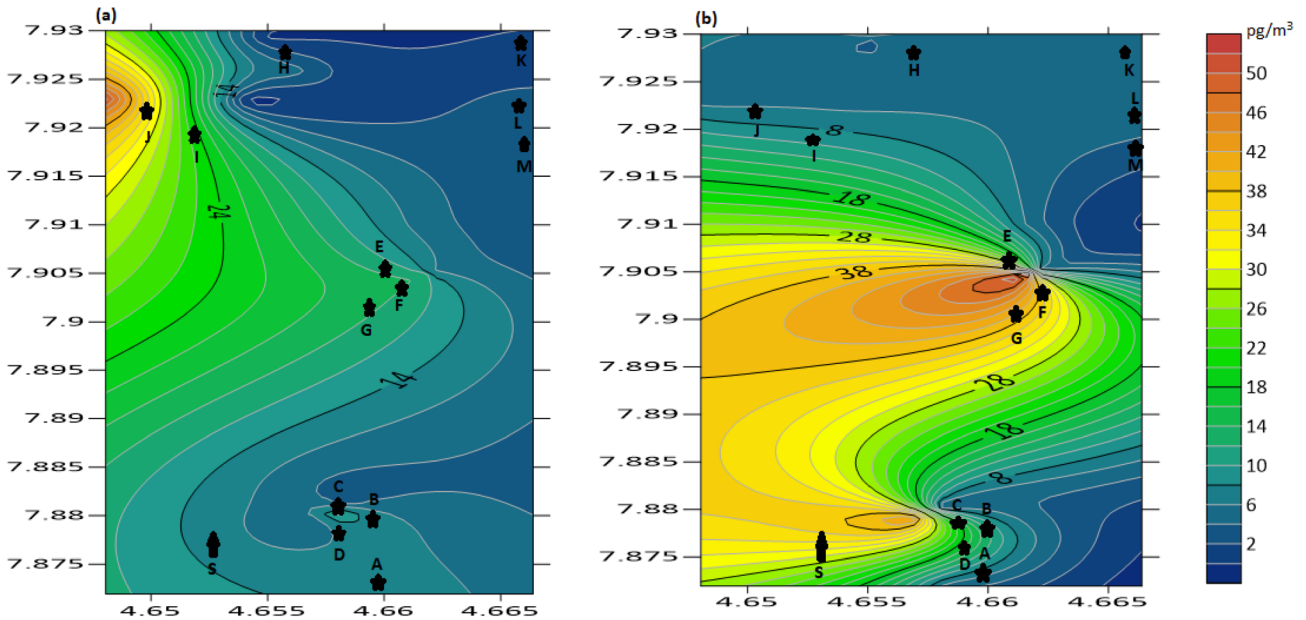

Fig. 8 Spatial distribution of PAHs: (a) dry season and (b) wet season.

Fig. 9 Wind rose diagram for (a) dry season and (b) wet season.

Temporal and spatial evaluation

Sampling was done between May and October for the wet season and between November and April for the dry season. As shown in Fig. 2 and 3, it was observed that the summation of PAH concentrations at different sampling points were higher during the dry season than in the wet season. This may be due to the hydrological conditions of the wet season, where the PAHs formed in the ambient air were easily precipitated and washed down by rainfall leading to lower PAH concentrations at some sampling locations in the wet season compared to the dry season.[20,29] Fig. 8a and b shows the concentration distribution of the PAHs around the recycling plant for the dry and wet seasons, respectively. The color legend indicates the mean concentration distribution in the air surrounding the recycling facility, and a decrease in the intensity of the colour from red to blue depicts decreasing mean concentrations from to 60 to 4 pg m^{-3} around the plant. The location of the recycling plant was denoted with S. In the wet season, a high-intensity coloration of red, yellow, and green was found in the southwestern and western regions of the recycling plant indicating high

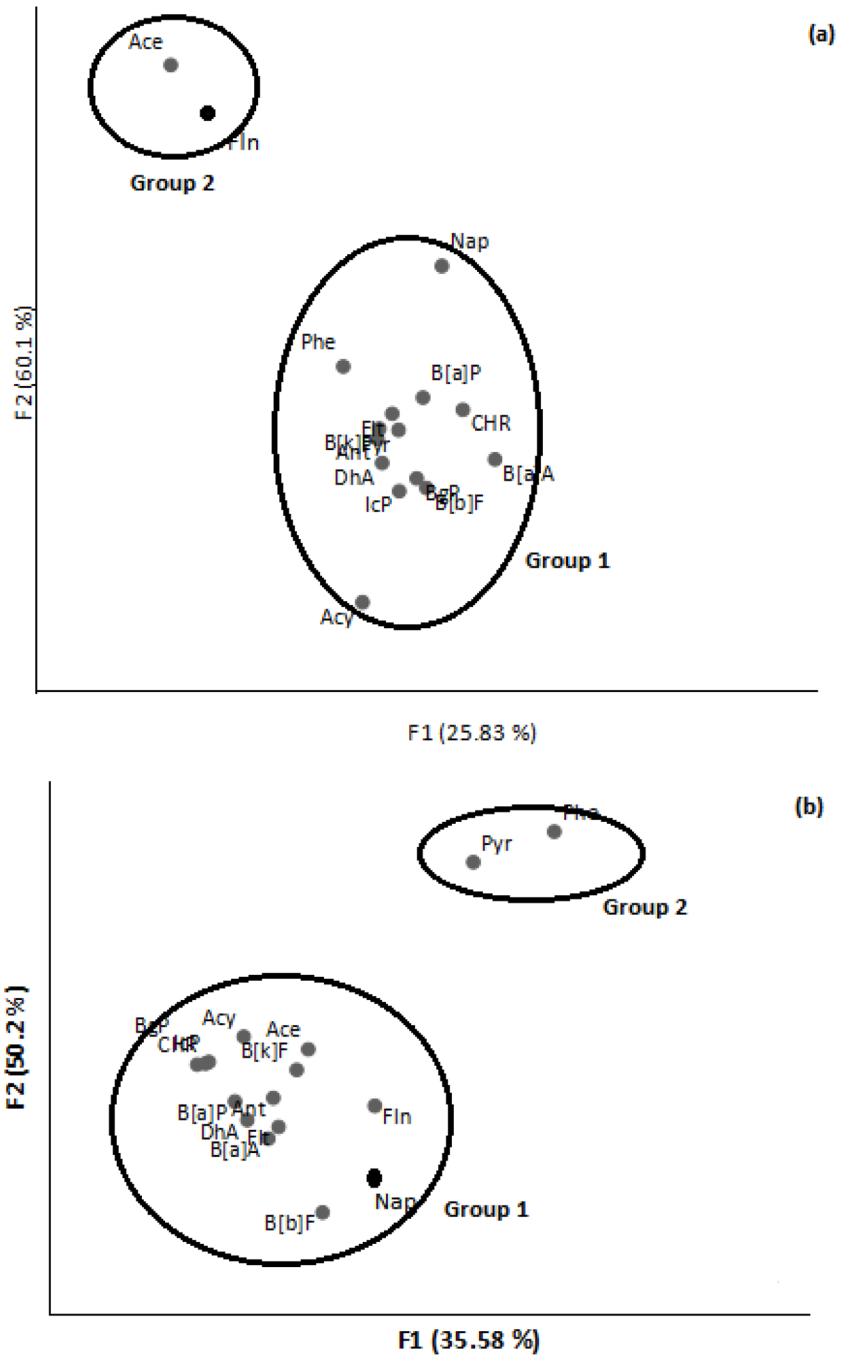

Fig. 10 Principal component analysis for (a) dry season and (b) wet season.

concentrations around these regions, which could be linked to the predominant wind direction as shown in the wind rose diagram in Fig. 9a. Additionally, a relatively high concentration of PAHs observed during this season could be associated with low mixing heights, inversions and relatively cold temperatures experienced during this season (Siudek, 2022).[30] In contrast, for the dry season, a high concentration was observed in the northeastern region of the recycling plant, indicating that the PAHs emitted were transported toward the northeastern direction of the plant, which can be linked to the predominant wind direction (Fig. 9b). Furthermore, the dry season is associated with a relatively high temperature, relatively deep mixing and increased dilution, which tend to favor the gas-phase transportation of PAHs (Siudek, 2022).[30]

Principal component analysis and hierarchical clustering analysis

Principal component analysis (PCA) and agglomerative hierarchical clustering analysis (HCA) (Fig. 10 and 11) are commonly employed to assess the source contributions of air pollutants, such as PAH compounds, to the surrounding air. The PCA was done using the nonlinear iterative least squares algorithm and the nearest neighbor linking with the Euclidean distance, and HCA was done using an agglomerative type of clustering.[31] In a PCA score plot, the variables with similar sources are generally located near to each other, while those with different sources are positioned farther apart.[19,20] The PCA variable plots for the dry and wet season are shown in Fig. 10a and b. Fig. 10a, which is the score plot for the dry season, has a cumulative variance of 85.93%, with the first principal component one (PC1) accounting for 25.83% of the total variance, while factor 2 (F2) accounts for 60.1% of the total variance. The PCA score plots and the dendrogram of HCA revealed that the data obtained can be assigned to two source groups. Most of the PAHs compounds investigated fell into group 1, indicating that they share the same source, which was the scrap iron and recycling industry. The data that fell into group two indicate additional sources contributing to the ambient PAHs in the area surrounding the company, such as vehicular emissions and other human activities. Similar to the dry season, Fig. 10b, which represents a score plot for the wet season, has a cumulative variance of 85.78% with principal component one (PC1) explaining 35.58% of the overall variation, and principal component two (PC2) accounting for 50.2%. Therefore, the variability of the ambient PAHs around the recycling plant can be explained. Two groups were observed from the PCA score plot and the dendrogram of HCA, with most of the data falling into group 1, indicating these PAHs shared the same source. A few PAH compounds fell into group 2, revealing that these PAHs likely had a source contribution from other sources around the vicinity of the industry.

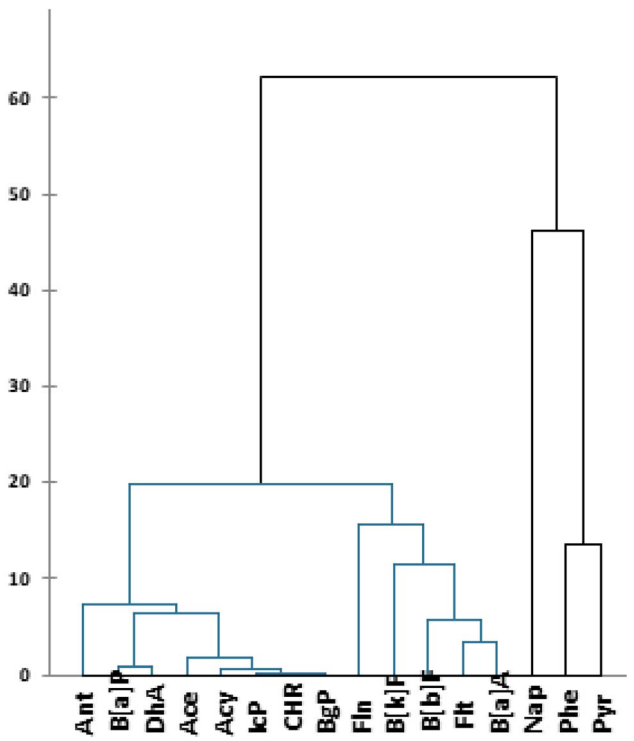

Fig. 11 Hierarchical tree cluster plot.

Diagnostic ratio analysis

The diagnostic ratio of some selected PAHs isomers is usually used for source apportionment of PAHs. The method used establishes a distinction between petrogenic and pyrolytic sources. The isomer ratios of Flu/(Flu + Pyr), Ant/(Ant + Phe) and BaA/(BaA + Chr) are commonly used to identify the possible source categories of PAHs (Wu *et al.*, 2014;[32] Kamal *et al.*, 2016[33]). An Ant/(Ant + Phe) ratio of 0.10 is used to differentiate between petrogenic (<0.10) and pyrogenic (>0.1) sources. A Flu/(Flu + Pyr) ratio is used to distinguish petroleum (<0.40) and (>0.50) combustion sources, while a Flu/(Flu + Pyr) ratio of 0.40–0.50 indicates petroleum combustion (traffic emission) (Menezes and Cardeal, 2012[34]). A BaA/(BaA + Chr) ratio < 0.20 indicates petrogenic origins, a ratio of >0.35 is indicative of combustion origins, while a ratio of 0.20–0.35 suggests mixed origins (Wu *et al.*, 2014;[32] Kamal *et al.*, 2016[33]). Tables 4 and 5 show the diagnostic ratios for the source identification of the PAHs for the dry and wet seasons. For the dry season, Flu/(Flu + Pyr) shows that around 70% of the samples were from combustion sources, while the remaining 40% were from petrogenic and traffic sources. The same trend was observed during the wet season using the same isomeric ratio, where 61% were from combustion sources and the remaining 39% were from petrogenic sources. The Ant/(Ant + Phe) ratio revealed that 92% of the samples were from a pyrogenic source, while the remaining 8% were from petrogenic sources for the dry season. For the wet season, the result shows that 85% of the samples were from a pyrogenic source, while the remaining 15% were from petrogenic sources. The BaA/(BaA + Chr) values revealed that 84% of the samples were from combustion sources and 16% were from petrogenic sources for the dry season. In the wet season, 70% were from combustion sources, 24% were from petrogenic sources, while 6% were from mixed petrogenic and combustion sources. Generally, the diagnostic ratio of PAHs revealed that

Table 4 Toxicity equivalent of PAHs for the dry season

PAHs	TEQ	A	B	C	D	E	F	G	H	I	J	K	L	M
Nap	0.001	0	0.0067	0	0.0233	0.01	0.0067	0.0133	0.0167	0.0067	0.0033	0.4067	0	0
Acy	0.001	0	0	0.0004	0.0014	0.0003	0	0.117	0.0011	0.0011	0.0011	0	0.0277	0.0003
Ace	0.001	0.0022	0.0583	0.0017	0.0022	0.0011	0.0578	0.005	0.005	0.0022	0.0544	0.0622	0.0033	0.0006
Fln	0.001	0.0776	0.0024	0.05	0.0486	0.0548	0.0005	0	0	0.001	0	0.0548	0.0024	0.0029
Phe	0.001	0.0013	0.0002	0	0.0011	0.0007	0.0216	0	0	0.0005	0.018	0.0016	0	0.0013
Pyr	0.001	0.0114	0.0002	0.0003	0.0007	0.0003	0.0005	0.0101	0.01	0.0002	0.0001	0.0008	0.0001	0.0001
Flt	0.001	0.0126	0.0004	0.0008	0.0004	0.0002	0.0114	0.0005	0.0009	0.0005	0	0	0	0.0002
Ant	0.001	0.0195	0.0016	0.0007	0.0005	0.0005	0.0013	0.0002	0.0002	0.0005	0.0202	0.0015	0.019	0.0009
B[*k*]F	0.1	0	0.97	0.06	0.1	0.05	0.03	0.04	0.04	0.05	0.02	0.06	0.06	0
B[*a*]P	1	0.1	0.5	11.4	8.9	10.2	0.2	0	0.1	0.3	10.3	0.4	0.2	0.7
CHR	0.1	1.11	0.09	1.03	1.01	0.99	1.06	1.05	0.95	1.02	0	0.02	0.08	1.02
B[*a*]A	0.01	0	0.008	0.923	0.006	0.107	0.095	0.005	0.007	0.092	0.008	0.002	0.114	0.104
IcP	0.1	0	0.01	0.07	0.08	0.06	0	0.08	0.09	1.13	0	0.04	0.97	0.02
B[*b*]F	0.1	0.01	0.07	0	0.05	1.05	0.07	0.98	0.06	0.02	0.05	0.03	0.97	1.03
DhA	1	0.1	0.6	0.4	0.4	0.3	0.3	0.7	8.8	0.5	0.4	0.4	9.1	0.5
BgP	0.01	0.004	0.009	0.003	0	0.003	0.002	0.096	0.091	0.104	0.003	0	0.001	0.11
TTEQ		1.4486	2.3268	13.9399	10.6242	12.8279	1.8568	3.0971	10.1719	3.2287	10.8781	1.4796	11.5475	3.4903

Table 5 Toxicity equivalent of PAHs for the wet season

PAHs	TEQ	A	B	C	D	E	F	G	H	I	J	K	L	M
Nap	0.001	0.0133	0.0233	0	0.35	0.02	0.02	0.0267	0.0233	0.0067	0.0067	0.0067	0.0133	0.0133
Acy	0.001	0.0006	0	0	0.0005	0	0	0	0	0.0021	0.0024	0.0024	0.0021	0.0013
Ace	0.001	0.0025	0	0	0	0.0025	0.0035	0.005	0.0025	0.003	0.003	0.004	0.003	0.0045
Fln	0.001	0.005	0.005	0.0032	0.0514	0.0055	0.0045	0.45	0.0059	0.0037	0.0032	0.0032	0.0032	0.0027
Phe	0.001	0	0	0.0014	0.0002	0	0.0003	0.0005	0.0005	0.0034	0.0166	0.019	0.0188	0.0183
Pyr	0.001	0.0009	0.0009	0.0104	0.0001	0.0005	0.0002	0.0003	0.0003	0.0122	0.0124	0.0124	0.0132	0.0003
Flt	0.001	0	0.0002	0.0097	0.0003	0.0012	0.0134	0.0135	0.0135	0.0002	0.0003	0.0002	0.0004	0.0003
Ant	0.001	0	0.0258	0	0	0.0008	0.0005	0.0005	0	0.0017	0.0007	0.0024	0.0017	0.001
B[*k*]F	0.1	1.22	0.04	0.88	0	0.02	0.02	0.01	0.01	0.05	0.08	0.03	0.05	0.97
B[*a*]P	1	0.4	0.4	0.8	8.8	12.1	0.3	0.1	0.1	0	0.6	0	0	0.7
CHR	0.1	0.03	0.03	0.01	0.05	0.05	0	0	0	0.08	0.03	0.08	0.06	0.01
B[*a*]A	0.01	0.004	0.001	0	0.091	0.001	0.117	0.12	0.12	0.011	0	0.006	0.007	0
IcP	0.1	0	0	0.07	1.2	0.03	0	0	0	0.06	0.08	0.03	0.05	0.08
B[*b*]F	0.1	1.12	1.12	0.04	0.02	0	1.15	1.66	1.66	0.01	0	0.01	0.04	0
DhA	1	0.4	10.9	0.4	0.3	12	0	0	0	0.1	0.3	0.2	0	0.5
BgP	0.01	0.001	0.001	0.001	0.002	0	0	0	0	0.001	0.007	0.003	0.003	0.003
TTEQ		3.1973	12.5472	2.2257	10.8655	24.2315	1.6294	2.3865	1.936	0.345	1.1423	0.4093	0.2657	2.3047

a larger percentage of the samples originated from pyrogenic and combustion sources, and a lower percentage originated from petrogenic sources, which indicates that the PAHs were from the combustion of cast iron with petroleum products. The results also show that an even smaller percentage of the PAHs were from vehicular emission. The results of this study are in line with the findings of Zhang *et al.* (2016),[35] who concluded that PAHs were mainly sourced from around the steel industry.

Risk assessment

Toxicity equivalent

Table 4 and 5 show the toxicity equivalent of the PAHs at the various sampling locations. It was observed that Bap and Dha had the highest toxicity equivalent for both seasons. This is greatly concerning as Bap has epigenotoxic, neurotoxic, and teratogenic tendencies. Studies have also shown that Dha has carcinogenic tendencies, as well as non-carcinogenic effects, such as nose, throat, and lungs irritations.[14,36] Flt had the lowest toxicity for the dry season, while Acy had the lowest toxicity for the wet season. The total toxicity equivalent (TTEQ) is the sum of the individual TEQs for the PAHs at each sampling location. During the dry season, TTEQ ranged from 1.45 to 13.94 pg m^{-3}, with an average value of 6.68 pg m^{-3}. In the wet season, TTEQ varied from 4.48 to 24.23 pg m^{-3}, with a mean value of 6.68 pg m^{-3}. This result could be linked to low temperatures, frequent inversions, a low mixing height, and relatively weaker wind occurring in this season, which increased the concentration of the MMW and HMW PAHs with a high toxicity equivalent (Siudek, 2022).[30]

Incremental life cancer risks and hazard quotient

The health risk assessments (ILCR and HQ) of human exposure to the PAHs around the company were carried out at various sampling points. The results obtained were compared with the permissible limits of 10^{-6} and 10^{-5}as stipulated by the USEPA

Table 6 ILCR for the wet and dry seasons

		A	B	C	D	E	F	G	H	I	J	K	L	M
Wet														
WHO	Children	3.19×10^{-6}	3.19×10^{-6}	6.38×10^{-6}	7.01×10^{-5}	9.64×10^{-5}	2.39×10^{-6}	7.97×10^{-7}	7.97×10^{-7}	0	4.78×10^{-6}	0	0	5.58×10^{-6}
WHO	Adult	2.85×10^{-6}	2.85×10^{-6}	5.69×10^{-8}	6.26×10^{-5}	8.61×10^{-5}	2.13×10^{-6}	7.12×10^{-7}	7.12×10^{-7}	0	4.27×10^{-6}	0	0	4.98×10^{-6}
USEPA	Children	2.2×10^{-8}	2.2×10^{-8}	4.4×10^{-8}	4.84×10^{-7}	6.65×10^{-7}	1.65×10^{-8}	5.5×10^{-9}	5.5×10^{-9}	0	3.3×10^{-8}	0	0	3.85×10^{-8}
USEPA	Adult	1.96×10^{-8}	1.96×10^{-8}	3.93×10^{-8}	4.32×10^{-7}	5.94×10^{-7}	1.47×10^{-8}	4.91×10^{-9}	4.91×10^{-9}	0	2.94×10^{-8}	0	0	3.44×10^{-8}
Dry														
WHO	Children	9.7×10^{-8}	3.98×10^{-6}	9.09×10^{-5}	7.09×10^{-5}	8.13×10^{-5}	1.59×10^{-6}	0	7.97×10^{-7}	2.39×10^{-6}	8.21×10^{-5}	3.19×10^{-6}	1.59×10^{-6}	5.58×10^{-6}
WHO	Adult	7.12×10^{-7}	3.56×10^{-6}	8.11×10^{-5}	6.33×10^{-5}	7.26×10^{-5}	1.42×10^{-6}	0	7.12×10^{-7}	2.13×10^{-6}	7.33×10^{-5}	2.85×10^{-6}	1.42×10^{-6}	4.98×10^{-6}
USEPA	Children	5.5×10^{-9}	2.75×10^{-8}	6.27×10^{-7}	4.89×10^{-7}	5.61×10^{-7}	1.1×10^{-8}	0	5.5×10^{-9}	1.65×10^{-8}	5.66×10^{-7}	2.2×10^{-8}	1.1×10^{-8}	3.85×10^{-8}
USEPA	Adult	4.91×10^{-9}	2.45×10^{-8}	5.59×10^{-7}	4.37×10^{-7}	5.01×10^{-7}	9.82×10^{-9}	0	4.91×10^{-9}	1.47×10^{-8}	5.05×10^{-7}	1.96×10^{-8}	9.82×10^{-9}	3.44×10^{-8}

Table 7 HQ for wet and dry seasons

	A	B	C	D	E	F	G	H	I	J	K	L	M
WET	19	19	38	420	577	14	5	5	0	29	0	0	33
	19	19	38	421	579	14	5	5	0	29	0	0	33
DRY	5	24	544	425	487	10	0	5	14	491	19	10	33
	5	24	545	426	488	10	0	5	14	493	19	10	33

and WHO, respectively. Table 6 shows the ILCR calculated for the wet and dry seasons. The average ILCR for the wet season using the WHO inhalation risk factor was 1.5×10^{-5} for children and an average value of 1.33×10^{-5} for adults. On average, these values exceeded the acceptable limit set by WHO. The sampling points D and E had ILCR values that exceeded the WHO allowable limit. However, some sampling points showed lower ILCR values than others, suggesting a reduced carcinogenic risk associated with human exposure to PAHs at these locations. A similar trend was observed during the dry season, with mean ILCR values of 2.7×10^{-5} for adults and 2.4×10^{-5} for children. However, using the USEPA inhalation risk factor, the average ILCR for children was 1.03×10^{-7}, while for adults, it was 9.17×10^{-8} during the wet season. In the dry season, the mean ILCR was 1.8×10^{-7} for children and 1.6×10^{-7} for adults. The difference in the ILCR for children and adults was related to differences in their body weight and inhalation rate. The obtained ILCR values using the USEPA inhalation risk factor were all lower than the USEPA stipulated permissible limit. The HQ values (Table 7) obtained at various sampling locations for both the dry and wet seasons were all greater than 1, indicating a high noncarcinogenic risk associated with contact with the PAHs around this vicinity.

Conclusion

This study investigated the spatial and temporal distribution of PAHs around a scrap iron and steel recycling facility. It also assessed the risk associated with human exposure to ambient air PAHs in the area surrounding the company. These findings indicate that scrap metal and recycling industries contribute to ambient levels of PAHs around their vicinity. Residences around the vicinity of the factories were exposed to higher concentrations of PAHs during the dry season. Although the limitation of the study includes a lack of access to the source concentration of PAHs from the factory, the predominant wind direction and wind speed, which are the meteorological parameters considered in this study, affected PAH variation around the factory. The risk analysis showed that the average incremental lifetime cancer risk (ILCR) exceeded that of the WHO guideline value of 10^{-5}. This indicates that for every 100 000 individuals exposed to these pollutants, considering the factors used for this study, there was a statistically likely expectation of one additional case of cancer. The study recommends that the government environmental monitoring agency should monitor the processes of these industries by ensuring strict compliance with environment standards. The government

should also ensure the usage of state-of-the-art air monitoring devices for controlling air pollution.

Conflicts of interest

The authors declare no conflict of interest.

Data availability

Raw data that support the findings are available from the corresponding author upon request.

Supplementary information (SI) is available. See DOI: https://doi.org/10.1039/d5ra05266a.

Acknowledgements

The authors express their gratitude to the Princess Nourah bint Abdulrahman University Researchers Supporting Project number (PNURSP2025R583), Princess Nourah bint Abdulrahman University, Riyadh, Saudi Arabia.

References

1 World Health Organization, *Factsheet on Ambient Air Quality and Health*. WHO, Geneva, Switzerland, 2018. Available from: http://www.who.int/news-room/fact-sheets/detail/ambient-(outdoor)-air-quality-and-health, Accessed 4 October 2024.

2 M. A. Lala, A. E. Taiwo, H. E. Lawal, O. A. Adesina and I. A. Igbafe, Particulate matter pollution over artisanal crude oil refining areas of Niger-Delta Nigeria: Spatiotemporal analysis, transport modelling and risk assessment, *Ain Shams Eng. J.*, 2024, 102654.

3 Clean Air Fund, *From pollution to solution in Africa's cities: The case for investing in air pollution and climate change together*, Clean Air Fund, Lagos, 2023, https://www.cleanairfund.org/clean-air-africas-cities/lagos/.

4 I. C. Nnorom and O. A. Odeyingbo, Electronic waste management practices in Nigeria, in *Handbook of Electronic Waste Management*, Butterworth-Heinemann, Oxford, 2020, pp. 323–354.

5 E. I. Ohimain, Scrap iron and steel recycling in Nigeria, *Greener J. Environ. Manag. Public Saf.*, 2013, **2**(1), 1–9.

6 O. Kehinde, O. J. Ramonu, K. O. Babaremu and L. D. Justin, Plastic wastes: Environmental hazard and instrument for wealth creation in Nigeria, *Heliyon*, 2020, **6**(10), e05131.

7 A. K. Lahiri and A. K. Lahiri, Production and working of metals and alloys, in *Applied Metallurgy and Corrosion Control: A Handbook for the Petrochemical Industry*, 2017, pp. 41–77.

8 K. O. Owoade, P. K. Hopke, F. S. Olise, L. T. Ogundele, O. G. Fawole, B. H. Olaniyi, O. O. Jegede, M. A. Ayoola and M. I. Bashiru, Chemical compositions and source identification of particulate matter (PM2.5 and PM2.5–10) from a scrap iron and steel smelting industry along the Ife–Ibadan highway, Nigeria, *Atmos. Pollut. Res.*, 2015, **6**(1), 107–119.

9 R. Liu, S. Ma, Y. Yu, G. Li, Y. Yu and T. An, Field study of PAHs with their derivatives emitted from e-waste dismantling processes and their comprehensive human exposure implications, *Environ. Int.*, 2020, **144**, 106059.

10 S. M. Mohammadi, B. Lorestani, S. Sobhan Ardakani, M. Cheraghi and M. K. Sadr, Source identification and health risk assessment of PAHs in surface soils from the vicinity of Arad-Kouh processing and disposal complex, Tehran, Iran, *Int. J. Environ. Anal. Chem.*, 2021, **103**(20), 9647–9660.

11 J. Xu, X. Peng, C. S. Guo, J. Xu, H. X. Lin, G. L. Shi and M. Tysklind, Sediment PAH source apportionment in the Liaohe River using the ME2 approach: A comparison to the PMF model, *Sci. Total Environ.*, 2018, **553**, 164–171.

12 A. Rabieimesbah, S. Sobhanardakani, M. Cheraghi and B. Lorestani, Concentrations, source identification and potential ecological and human health risks assessment of polycyclic aromatic hydrocarbons (PAHs) in agricultural soils of Hamedan County, West of Iran. Soil and Sediment Contamination, *Soil Sediment Contam.*, 2023, **33**(4), 482–506.

13 W. G. Luo, Identification of sources of polycyclic aromatic hydrocarbons based on concentrations in soils from two sides of the Himalayas between China and Nepal, *Environ. Pollut.*, 2016, **212**, 424–432.

14 O. A. Adesina, R. Opara, A. J. Adewale, M. A. Lala and J. A. Sonibare, Characterization of polycyclic aromatic hydrocarbon from open burning of disposable COVID-19 facemask: Spatial distribution and risk assessment, *Arabian J. Chem.*, 2024, **17**(4), 105721.

15 L. T. Ogundele, O. K. Owoade, F. S. Olise and P. K. Hopke, Source identification and apportionment of PM2.5 and PM2.5−10 in iron and steel scrap smelting factory environment using PMF, PCFA and UNMIX receptor models, *Environ. Monit. Assess.*, 2016, **188**, 1–21.

16 F. Solademi and S. Thompson, Spatial analysis of heavy metal emissions in residential, commercial and industrial areas adjacent to a scrap metal shredder in Winnipeg, Canada, *J. Geosci. Environ. Protect.*, 2020, **8**(5), 359–386.

17 M. Mpewo, S. Kizza-Nkambwe and J. S. Kasima, Heavy metal and metalloid concentrations in agricultural communities around steel and iron industries in Uganda: Implications for future food systems, *Environ. Pollut. Bioavailability*, 2023, **35**(1), 2226344.

18 J. A. Adeniran, B. T. Ogunlade, E. T. Odediran, R. O. Yusuf and J. A. Sonibare, Polycyclic aromatic hydrocarbons within the vicinity of a scrap-iron smelting plant: Indoor–outdoor and seasonal pattern, source, and exposure risk assessment, *Int. J. Environ. Health Res.*, 2024, **35**(8), 2103–2121.

19 O. A. Adesina, J. A. Sonibare, P. N. Diagboya, A. Adejuwon, T. Famubode and J. O. Bello, Periodic characterization of alkyl-naphthalenes in stack gas and ambient air around a medical waste incinerator, *Environ. Sci. Pollut. Res.*, 2017, **24**, 21770–21777.

20 O. A. Adesina, J. A. Sonibare, P. N. Diagboya, J. A. Adeniran and R. O. Yusuf, Spatiotemporal distributions of polycyclic

aromatic hydrocarbons close to a typical medical waste incinerator, *Environ. Sci. Pollut. Res.*, 2018, **25**, 274–282.

21 K. Pozo, T. Harner, M. Shoeib, R. Urrutia, R. Barra, O. Parra and S. Focardi, Passive-sampler derived air concentrations of persistent organic pollutants on a North–South transect in Chile, *Environ. Sci. Technol.*, 2004, **38**(24), 6529–6537.

22 O. A. Adesina, O. M. Kolawole, M. A. Lala, M. G. Omofoyewa and A. I. Igbafe, Characterization and risk assessment of polycyclic aromatic hydrocarbons from the emission of different power generator, *Heliyon*, 2024, **10**(11), e25984.

23 T. Harner, M. Mitrovic, L. Ahrens and J. Schuster, Characterization of PUF disk passive air samplers for new priority chemicals, A review, *Organohalogen Compd.*, 2014, **76**(1), 442–445.

24 T. Harner, K. Su, S. Genualdi, J. Karpowicz, L. Ahrens, C. Mihele, J. Schuster, J. P. Charland and J. Narayan, Calibration and application of PUF disk passive air samplers for tracking polycyclic aromatic compounds (PACs), *Atmos. Environ.*, 2013, **75**, 123–128.

25 United States Environmental Protection Agency (USEPA), *Exposure Factors Handbook Edition (Final)*, US Environmental Protection Agency, Washington, DC, 2011, EPA/600/R-09/052F.

26 V. V. Khaparde, A. D. Bhanarkar, D. Majumdar and C. V. C. Rao, Characterization of polycyclic aromatic hydrocarbons in fugitive PM10 emissions from an integrated iron and steel plant, *Sci. Total Environ.*, 2016, **562**, 155–163.

27 Y. Zhang, H. Zheng, L. Zhang, Z. Zhang, X. Xing and S. Qi, Fine particle-bound polycyclic aromatic hydrocarbons (PAHs) at an urban site of Wuhan, central China: Characteristics, potential sources and cancer risks apportionment, *Environ. Pollut.*, 2019, **246**, 319–327.

28 R. Rostami, A. Zarei, B. Saranjam, H. R. Ghaffari, S. Hazrati, Y. Poureshg and M. Fazlzadeh, Exposure and risk assessment of PAHs in indoor air of waterpipe cafés in Ardebil, Iran, *Build. Sci.*, 2019, **155**, 47–57.

29 J. Lv, J. Xu, C. Guo, Y. Zhang, Y. Bai and W. Meng, Spatial and temporal distribution of polycyclic aromatic hydrocarbons (PAHs) in surface water from Liaohe River Basin, northeast China, *Environ. Sci. Pollut. Res.*, 2014, **21**, 7088–7096.

30 P. Suidek, Seasonal distribution of PM2.5-bound polycyclic aromatic hydrocarbons as a critical indicator of air quality and health impact in a coastal-urban region of Poland, *Sci. Total Environ.*, 2022, **827**, 154375.

31 H. Gao, Y. Ni, H. Zhang, L. Zhao, N. Zhang, X. P. Zhang, Q. Zhang and J. P. Chen, Stack gas emissions of PCDD/Fs from hospital waste incinerators in China, *Chemosphere*, 2009, **77**, 634–639.

32 S. P. Wu, B. Y. Yang, X. H. Wang, C. S. Yuan and H. S. Hong, Polycyclic aromatic hydrocarbons in the atmosphere of two subtropical cities in southeast China: Seasonal variation and gas/particle partitioning, *Aerosol Air Qual. Res.*, 2014, **14**, 1232–1246.

33 A. Kamal, J. Syed H, J. Li, G. Zhang, A. Mahmood and R. Malik N, Profile of atmospheric PAHs in Rawalpindi, Lahore and Gujranwala districts of Punjab province (Pakistan), *Aerosol Air Qual. Res.*, 2016, **16**, 1010–1021.

34 H. C. Menezes and Z. L. Cardeal, Study of polycyclic aromatic hydrocarbons in atmospheric particulate matter of an urban area with iron and steel mills, *Environ. Toxicol. Chem.*, 2012, **31**, 1470–1477.

35 J. Zhang, C. Zhan and H. Liu, Characterization of Polycyclic Aromatic Hydrocarbons (PAHs), Iron and Black Carbon within Street Dust from a Steel Industrial City, Central China, *Aerosol Air Qual. Res.*, 2016, **16**, 2452–2461.

36 B. Bukowska, K. Mokra and J. Michałowicz, Benzo[a] pyrene—Environmental occurrence, human exposure, and mechanisms of toxicity, *Int. J. Mol. Sci.*, 2022, **23**(11), 6348.